*Research Article*

http://dx.doi.org/10.21060/cis.2015.331

# Synthesis, spectroscopy and structural analysis of Technetium and Rhenium nitrosyl complexes.

**Terrence Nicholson*[a,b,c], Esther Chun[b] ,Ashfaq Mahmood[b] , Peter Mueller[a] , Alan Davison[a] and Alun G. Jones[b]**

[a]Department of Chemistry, Massachusetts Institute of Technology, Cambridge, MA. [b]Department of Radiology, Harvard Medical School, Boston, MA. [c]Simmons College, Boston, MA.

*E-mail: terrence.nicholson@simmons.edu

*Received: June 04, 2015; accepted: August 03, 2015*

**Abstract:** Here we report an overview of our synthetic, spectroscopic and structural studies of technetium and rhenium nitrosyl complexes. We review the results from various notes and short papers reported over the past 15 years and discuss their significance in terms of radiopharmaceutical design.

A single new complex is reported, the $Re^{I}$-NO complex [$Re^{I}Cl_2$(NO)(py-N(Et)-py)], in which the tridentate ligand di-(2-picolyl)(N-ethyl)amine, (py-N(Et)-py), is coordinated in a meridional manner. This complex was synthesized from the reaction of the $Re^{I}$-nitrosyl complex $ReCl_2(NO)(NCMe)_3$] and the neutral tri-amine ligand py-N(Et)-py in methylene chloride under argon. The bright red species was isolated chromatographically and recrystallized from $CH_2Cl_2$/MeOH under diethylether. The infrared spectrum displays ν(N=O) at 1668 $cm^{-1}$. The ESI mass spectrum displays the parent peak, [ReCl(NO)(py-N(Et)-py)]$^+$, at 479 m/z; and a second peak from [$ReCl_2$(NO)(py-N(Et)-py)]$^+$ at 414 m/z.

The X-ray crystal structure established this species to contain mutually trans-chloride ligands, with the tridentate ligand coordinated in a meridional manner. The nitrosyl ligand displays multiple bonding throughout, with a Re-N bond length of 1.742 (2) Å and nitrogen-oxygen bond length of 1.202(3) Å. The Re-N-O bond angle is nearly linear, at 177.3(2)°. There is significant deviation from ideal octahedral geometry, mainly due to the small bite angle of the tridentate ligand. The Re-N bond length to the amine nitrogen trans- to the nitrosyl nitrogen is significantly longer than the bonds to the two aromatic amine nitrogens, as expected. {2.231(2)Å vs 2.085(2)Å and 2.091(2) Å}. A review of literature values for nitrosyl complexes with various ligands bound to the coordination site *trans*- to the nitrosyl group shows only minor variations in the M-N-O bond angle.

**Keywords:** *Rhenium*, *nitrosyl*, *technetium* .

## 1. INTRODUCTION

Rhenium nitrosyl chemistry has received increased scrutiny recently, pertaining to hydrogen related catalyses. Technetium, rhenium's second row congener, is radioactive. Its long-lived isotope $^{99}$Tc, is a weak beta emitter with a half-life of 211,000 years, which essentially prohibits analogous studies in catalysis. Technetium's short-lived isotope $^{99m}$Tc, (half-life of about 6 hours) is used extensively in SPECT-based (Single-Photon Emission Computed Tomography) diagnostic imaging agents for nuclear medicine. Technetium-99m is used in 20 million diagnostic nuclear medical procedures every year. Technetium-nitrosyl complexes for application in radiopharmaceutical development have been largely overlooked.

Both PET (positron emission tomography) and SPECT imaging probes contribute to modern clinical medicine, particularly in cardiology, oncology and neurology. It should be emphasized that the installed base of SPECT-capable cameras is still far larger than that for PET devices, and further, PET is severely limited in its utility and its availability. In the United States, in 2008, SPECT devices outnumbered PET by over 12,000 to 1,000 [1,2]. Furthermore, the continuing advancement in SPECT imaging technologies, particularly those designed for specific procedures, is proceeding rapidly [3-7]. Thus the role of SPECT imaging agents, particularly those incorporating Tc-99m, remains very important in providing cost effective clinical information that is readily accessible at all times to a wide population. These facts continue to make exploration of the basic coordination chemistry of technetium of prime importance, in spite of the US federal funding agencies' lack of insight and perspective in this matter.

The search for new SPECT imaging probes lies at an intersection of inorganic, organic and medicinal chemistry. Critical to the development of new imaging agents is the availability and utility of core structural building blocks upon which the rest of the molecule is built. For SPECT imaging agents, the technetium-core is essential to designing new and novel complexes, and the availability of new metal-cores is thus important. A transition metal core is defined here as a recurrent molecular foundation of inherent structural and redox stability containing the metal ion upon which the molecule is constructed. The remain-

ing coordination sites of the metal ion are available for substitution in order to complete the molecular geometry and supplement the stability of the metal core. Through choice and orientation of donor groups in the chelating ligand design, the complex is provided with additional stability as well as a means of integrating or attaching specific targeting pendant pharmacophores. Taken as a whole, the metal core, in conjunction with an appropriate chelating ligand and pharmacophore, is what determines the overall charge, shape, lipophilicity and consequently the utility of the chelated metal complex as an imaging probe.

The significance of novel inorganic chemistry that can further radiopharmaceutical design of new technetium complexes can be traced back to the initial identification of the $Tc^{V}O$ core and its subsequent use in the design of clinically useful agents such as $^{99m}TcO^{V}$-HMPAO, $^{99m}TcO^{V}$-ECD, $^{99m}TcO^{V}$-$MAG_3$, and $^{99m}TcO^{V}$-TRODAT; agents that are currently used world-wide in the diagnostic nuclear medicine clinics.[8,9] Similarly, several new preclinical agents currently under evaluation can be attributed to the impact of identifying the metal-*tri*carbonyl $\{M^{I}(CO)_3\}$ core as a viable stable metal core[10-15]. This $\{Tc^{I}(CO)_3\}$ core has been under intense scrutiny for the past decade, with new preclinical agents currently under development [16-18]. The list of component cores in technetium imaging agents currently employed in the clinic is short. The most widely utilized is the Tc(V)-oxo core, which is found in a number of imaging agents. The Tc(V)-oxo core is distinguished by its stability and its ability to accommodate a variety of different functional groups in its four available coordination sites. This allows its chemical and biological properties to be readily manipulated with various chelating ligands designed to supplement the metal -oxo core. Among the low oxidation state species, the Tc(I)-core is found in $\{Tc^{I}$-$(MIBI)_6\}$, which is inert to ligand substitution. A more structurally versatile Tc(I) species is the Tc(I)-tricarbonyl core, $\{Tc^{I}(CO)_3\}$, which retains three carbonyl groups locked in a *facial* arrangement, allowing ligation at its remaining three coordination sites. This Tc(I) core has been under intense scrutiny for the past decade, with many derivatives synthesized, characterized and evaluated in preclinical studies. Its versatility however is limited in that only three *facial* coordination sites are available for ligation to complete the metal octahedral geometry. This restriction greatly reduces the utility of the core in radiopharmaceutical design.

Our recent efforts in developing new technetium chemistry led us to identify the M-nitrosyl {M-NO, where M = Re or Tc} as a novel core worth further investigation. While some chemistry with this core has been reported [19], it has yet to be exploited in the design of new technetium radiopharmaceuticals, mainly due to the lack of useful precursors *and* a thorough understanding of the ligand preferences required for synthesis of stable metal complexes. To date the Tc-NO core has been identified almost exclusively in formal [+2] or [+1] oxidation states [20]. The *de facto* synthetic precursor for technetium nitrosyl chemistry has been $(Bu_4N)[Tc^{II}(NO)Cl_4]$, [1] a Tc(II) species that is five coordinate and contains easily replaceable chloride ligands, making it very reactive in ligand exchange reactions. However, a major drawback with respect to radiopharmaceutical chemistry is that this $Tc^{II}$-NO precursor is routinely reduced to products containing the $Tc^{I}$-NO core, even under ambient reaction conditions. Simple ligand exchange reactions under mild reaction conditions are invariably complicated by concomitant redox chemistry that lowers yields and creates by-products.

The rhenium(II) nitrosyl complex $(Bu_4N)_2[Re^{II}(NO)Cl_5]$, [21], closely related to $(Bu_4N)[Tc^{II}(NO)Cl_4]$, has been reported, but it has yet to be thoroughly explored in reactions relevant to radiopharmaceutical utility. Periodic trends suggest technetium and rhenium chemistry will closely parallel each other, however this trend does not generally hold with redox reactions. The development of parallel technetium- and rhenium-nitrosyl chemistry and identification of analogous complexes is necessary from a radiopharmaceutical chemistry perspective. Structural analogs of technetium complexes with cold rhenium are important in various chromatographic characterization studies, which are not practical from a waste management perspective using the long-lived isotope $^{99}$Tc. Furthermore, *in vitro* biological assays such as competitive receptor binding studies, where $^{3}$H-ligands are used with non-radioactive Re-complexes because $\beta^-$ emissions from $^{99}$Tc-complexes complicate the analysis. We thus embarked on a cursory exploration of substitution reactions of technetium and rhenium nitrosyl complexes in oxidations states (I) and (II). Here we summarize our results, most of which have been previously presented in notes and short papers. We discuss the big picture, and how this chemistry might be utilized in radiopharmaceutical development. Additionally, a single new compound, $[ReCl_2(NO)$(py-N(Et)-py)], a Re(I) nitrosyl complex with a tridentate amine ligand is presented.

## 2. EXPERIMENTAL

Reagents and solvents were used as received unless otherwise stated. The technetium nitrosyl precursor $(Bu_4N)[Tc(NO)Cl_4]$ was prepared by method of Thornback *et al.*[22] $ReCl_2(NO)(NCMe)_3]$ was prepared by method of Jaing. [23] Routine infrared spectra were obtained on a Perkin–Elmer Spectrum One FT-IR Spectrometer. Mass spectra were recorded on a Bruker Daltonics APEXII 3 Tesla Fourier Transform Mass Spectrometer (Ion Cyclo-tron Resonance Mass Spectrometer). See Table 1 for summation of X-ray crystallographic data set collection and refinement parameters.

## 3. RESULTS AND DISCUSSION

**$[ReCl_2(NO)$(py-N(Et)-py)]** - A 0.025g sample of di-(2-picolyl)(N-ethyl)amine (py-N(Et)-py) (0.098 mmol) and 0.045g $ReCl_2(NO)(NCMe)_3]$ (0.012 mmol) were combined in 40 mL of methylene chloride under argon. Stir at RT for 48 h. Chromatograph the resulting golder-orange solution on silica, eluting with

5% methanol in methylene chloride. Two mobile bands of purple and cherry-red color were isolated. The red band produced red crystals when layered with diethylether. Yield 12 mg (22 %). CCDC 1027523.

IR(neat) ($cm^{-1}$): 1668, ν(N=O), (vs). ESI(+) Mass Spectrum (m/z): 414, $[ReCl_2(NO)(py\text{-}N(Et)\text{-}py)]^+$; $[ReCl(NO)(py\text{-}N(Et)\text{-}py)]^+$, 479 m/z.

*For details of the synthetic procedures and structural analyses, please see the following refernces:*

| **Compounds** | **Reference** |
|---|---|
| $[ReBr_2(NO)(NCMe)\{py\text{-}NH\sim N(\text{-}py)_2\}]$ | [24] |
| $[Re(NO)\{py\text{-}NH\text{-}N(\text{-}py)_2\}](BPh_4)_2$ | [25] |
| $[TcCl_2(NO)(py\text{-}N(Et)\text{-}py)]$ | [24] |
| $[TcCl(NO)(py\text{-}N(Et)\text{-}py)(PPh_3)]Cl$ | [24] |
| $[TcCl(NO)(py\text{-}NH\text{-}NH\text{-}py)]Cl$ | [24] |
| $[TcCl(NO)(py\text{-}NH\text{-}NH\sim py)(PPh_3)]Cl$ | [24] |
| $[TcCl(NO)(Spy)(PPh_3)_2]$ | [26] |
| $[Tc(NO)(Spy)_2(PPh_3)]$ | [26] |
| $[TcCl_2(NO)(HN{=}NC_5H_4N)(PPh_3)]$ | [27] |
| $[TcCl_2(NO)(py)_3]$ | [28] |
| $[TcCl_2(NO)(Ph_2P\text{-}N(pr)\text{-}PPh_2)]$, (*fac*) | [29] |
| $[TcCl_2(NO)(Ph_2P\text{-}N(pr)\text{-}PPh_2)]$, (*mer*) | [29] |

**Table 1**

| | |
|---|---|
| Chemical formula | $C_{14}H_{17}Cl_2N_4ORe$ |
| Chemical formula weight | 514.41 |
| Space group crystal system | triclinic |
| Space group | P-1 |
| Cell length a | 7.4116(5) |
| Cell length b | 8.6967(5)(5) |
| Cell length c | 13.3915(10) |
| Cell angle alpha | 86.631(3) |
| Cell angle beta | 75.7804(19) |
| Cell angle gamma | 72.3119(17) |
| Cell volume | 797.05(9) |
| Cell formula units Z | 2 |
| Cell measurement -temperature | 100(2) |
| Cell measurement -reflns used | 9650 |
| cell measurement –theta min, max | 2.46, 31.63 |
| exptl crystal description | block |
| exptl crystal colour | red |
| exptl crystal density diffrn | 2.143 |
| exptl crystal F 000 | 492 |
| exptl crystal size -max, mid, min | 0.280, 0.190, 0.110 |
| exptl absorpt coefficient -mu | 7.964 |
| shelx estimated absorpt -T min, max | 0.214, 0.475 |
| exptl absorpt correction type | multi-scan |
| exptl absorpt correction -T min, max | 0.115142, 0.214051 |
| exptl absorpt process details | SADABS (Sheldrick, 2009) |
| diffrn radiation wavelength | 0.71073 |
| diffrn radiation type | MoK\α |
| diffrn measurement method | ϕ and ω scans |
| diffrn reflns number | 5341 |
| diffrn reflns limit -h min, max | -10, 10 |
| diffrn reflns limit -k min, max | -12, 12 |
| diffrn reflns limit -l min, max | 0, 19 |
| diffrn reflns theta –min, max | 1.569, 31.708 |
| reflns number -total | 5341 |
| reflns number -gt | 5212 |
| reflns threshold expression | I > 2\σ(I) |
| refine ls number reflns | 5341 |
| refine ls number parameters | 201 |
| refine ls number restraints | 0 |
| refine ls R factor -all | 0.0207 |
| refine ls R factor -gt | 0.0200 |
| refine ls wR factor -ref | 0.0527 |
| refine ls wR factor -gt | 0.0523 |
| refine ls goodness of fit -ref | 1.046 |

*Instrumentation - Bruker X8 Kappa DUO four-circle diffractometer, Bruker APEX2 CCD. The instrument was purchased with the help of funding from the National Science Foundation (NSF) under Grant Number CHE-0946721. Refine Special Details - Refined as a 2-component non-merohedral twin. Similar ADP and Hirshfeld restraints applied to all atoms.*

## 4. DISCUSSION

The synthesis of the nitrosyl precursor $(Bu_4N)[Tc^{II}(NO)Cl_4]$ involves the reductive nitrosylation of the Tc(V)-oxo complex $(Bu_4N)[Tc^{V}OCl_4]$ with excess hydroxylamine-HCl in methanol [1]. This five coordinate, air stable Tc(II)-NO complex is very

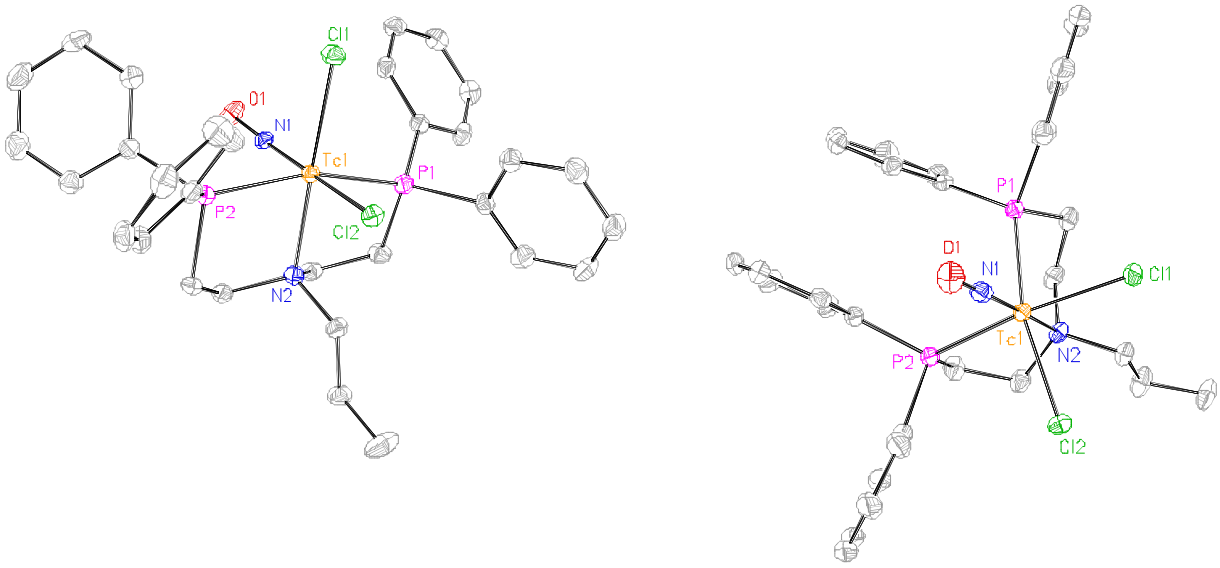


**Figure 1.** ORTEP diagrams of the $Tc^{I}$-NO *meridional* $[Tc^{I}Cl_2(NO)(PNP)]$ and *facial* $[Tc^{I}Cl_2(NO)(PNP)]$ complexes.

reactive with most conventional ligand types at ambient reaction conditions, seemingly making it well suited for ligand evaluation screening towards the development of imaging agents. However preliminary results proved problematic, with very poor yields and mixtures of products that were consistently unstable. All products identified from reactions with this precursor were reduced Tc(I)-NO species.

Reactions of $(Bu_4N)[Tc^{II}(NO)Cl_4]$ with stoichiometric quantities of the tridentate *bis*-phosphine-amine ligand $Ph_2PCH_2CH_2N(Et)CH_2CH_2PPh_2$, {PNP} in various solvents and at various temperatures, yielded complex mixtures of products as determined by infrared spectroscopy and chromatography. Complicating this scheme was the fact that these products were unstable, reacting further upon sitting in solution. It became apparent that the Tc (II) oxidation state of $(Bu_4N)[Tc^{II}(NO)Cl_4]$ was a significant complicating factor in these reactions, especially with redox active ligands like the phosphines in the tridentate PNP ligands. The PNP ligands in these reactions are both, facilitating the anticipated ligand exchange reaction and serving as a reducing agent, in converting the Tc(II)-precursor to the Tc(I) products. The *mer*- and *fac*- isomers of the Tc(I) complex $[Tc^{I}Cl_2(NO)(PNP)]$ are the major products isolated from these reactions in acetonitrile and methanol respectively, although yields in both reactions were very low. The X-ray crystallographic studies of these two complexes confirm the presence of linear nitrosyl groups, which are displayed below as ORTEP diagrams in Figure 1. The Tc-N-O bond angles for the *facial* complex is 177.9 (4)° and for the *meridional* complex is 173.0(4)°. This 5° difference in bond angle likely reflects the difference in ligands *trans*- to the $Tc^{I}$-NO core, which are an aliphatic amine and a chloride, respectively. These results leads to the conclusion that the redox active $Tc^{II}$-NO precursor $(Bu_4N)[Tc^{II}(NO)Cl_4]$ creates significant synthetic complications, and that better yields of stable products would come from a $Tc^{I}$-NO precursor.

The air stable $Tc^{I}$-NO complex $[Tc^{I}Cl_2(NO)(HOMe)(PPh_3)_2]$ was synthesized from $(Bu_4N)[Tc^{II}(NO)Cl_4]$. It contains easily replaceable methanol and chloride ligands, which makes this Tc (I)-NO complex well suited for further evaluation in imaging probe design. Syntheses using this Tc(I) precursor proved effective, giving higher yields and stable $Tc^{I}$-NO products, by effectively eliminating the complicating redox chemistry associated with the Tc(II) precursor $(Bu_4N)[Tc^{II}(NO)Cl_4]$. The reaction sequence depicted in Figure 2 below shows the redox reactions involved in converting pertechnetate to a $Tc^{I}$-NO precursor.

Reactions of the Tc(I) precursor $[Tc^{I}Cl_2(NO)(HOMe)(PPh_3)_2]$ with a series of bi-, tri-, tetra- and pentadentate ligands give promising results. Though far from exhaustive, these preliminary studies suggest that the structurally versatile family of polyamine ligands form stable complexes and warrant further eval-


**Figure 2**: Sequential reduction reactions necessary to generate the Tc(I)-NO precursor $[Tc^{I}Cl_2(NO)(HOMe)(PPh_3)_2]$ from pertechnetate.

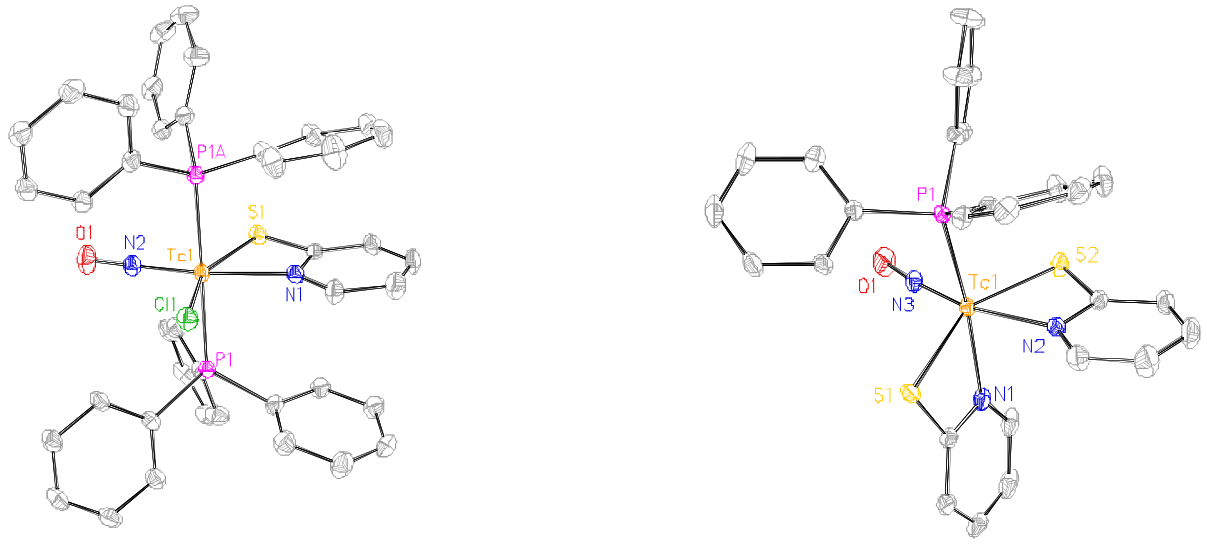


**Figure 3 –** ORTEP diagrams of the $Tc^{I}$-NO mercaptopyridine complex $[Tc^{I}Cl(NO)(Spy)(PPh_3)_2]$ and the $Tc^{I}$-NO *bis*-mercaptopyridine complex $[Tc^{I}(NO)(Spy)_2(PPh_3)]$.

uation in radiopharmaceutical design and development.

Using the $Tc^{I}$-NO precursor $[Tc^{I}Cl_2(NO)(HOMe)(PPh_3)_2]$, with stoichiometric amounts of the bidentate ligand 2-mercaptopyridine and a proton scavenger gives good yields of the structurally characterized Tc(I) complex $[Tc^{I}Cl(NO)(Spy)(PPh_3)_2]$. Similar reaction of $[Tc^{I}Cl_2(NO)(HOMe)(PPh_3)_2]$ and an excess of 2-mercaptopyridine and proton scavenger gives high yields of the *bis*-mercaptopyridine adduct $[Tc^{I}(NO)(Spy)_2(PPh_3)]$. The ORTEP diagrams of these two complexes are shown in Figure 3 below. In both structures there is significant deviation from octahedral geometry that is a result of distortion introduced by the small bite angle of the bidentate ligand. Employing this $Tc^{I}$-NO precursor significantly reduces the difficulties encountered earlier when employing the $Tc^{II}$-NO precursor $(Bu_4N)[Tc^{II}(NO)Cl_4]$. In both of these reactions of the $Tc^{I}$-NO precursor, no chromatographic purification was needed, yielding X-ray quality crystals (Figure 3).

To directly compare the reactions of the $Tc^{I}$-NO and $Tc^{II}$-NO precursors, each was reacted with the neutral, tridentate ligand *bis*-2-picolyl(N-ethyl)amine. Reaction with $(Bu_4N)[Tc^{II}(NO)$

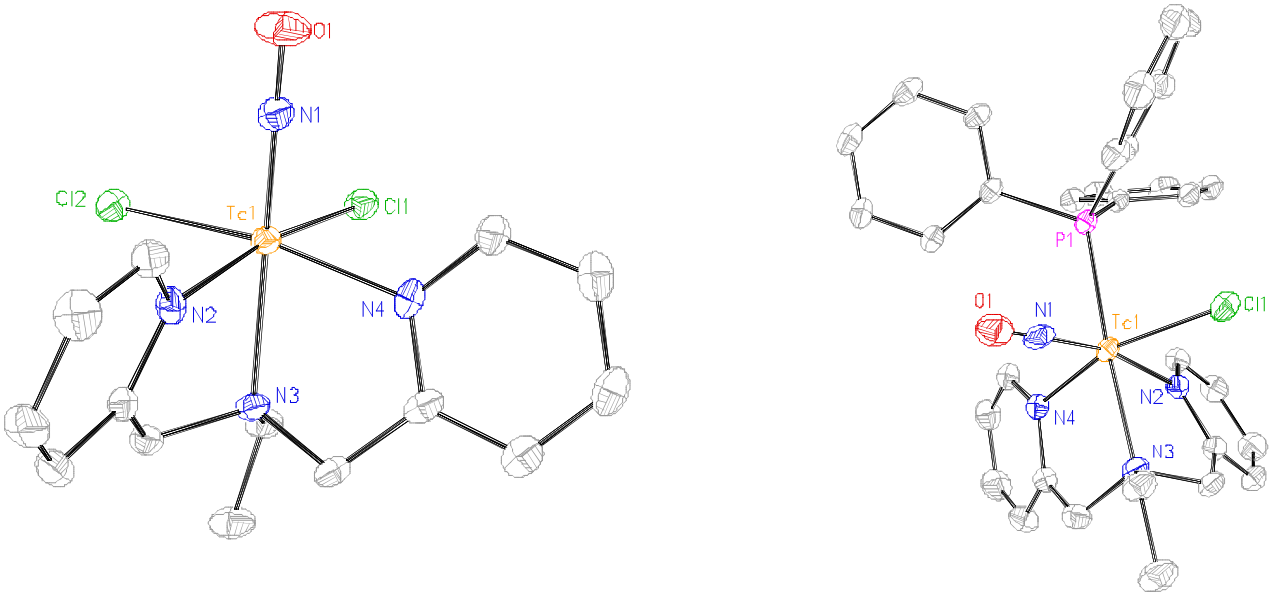


**Figure 4 –** ORTEP diagrams of the $Tc^{I}$-NO complex $[Tc^{I}Cl_2(NO)(py\text{-}N(Et)\text{-}py)]$ in which the N3 ligand is coordinated in a facial manner, and the cationic $Tc^{I}$-NO complex $[Tc^{I}Cl(NO)(PPh_3)(py\text{-}N(Et)\text{-}py)]^{+}$.

$Cl_4$] again gave a complex mixture of products that required chromatographic separation. The predominant stable product isolated was the neutral Tc(I) complex [$Tc^ICl_2$(NO)(py-N(Et)-py)], which incorporates the tridentate ligand in a *facial* orientation, and was isolated in 23% yield. This same tridentate ligand, when reacted with the reduced $Tc^I$-NO precursor [$Tc^ICl_2$(NO)(HOMe)($PPh_3$)$_2$], gave a much higher, 47% yield of the cationic complex [$Tc^ICl$(NO)($PPh_3$)(py-N(Et)-py)]Cl. Here too, the tridentate ligand is coordinated in a *facial* orientation, however, given the presence of $PPh_3$ in the precursor, the isolated product retains a phosphine coligand coordinated *trans*- to the aliphatic amine. The charge difference found in these two complexes is due to the retention of a $PPh_3$ in the latter product and its absence in the former. ORTEP diagrams of these two complexes are illustrated in Figure 4. (Note that the chloride ion from the cationic species has been omitted for clarity.)

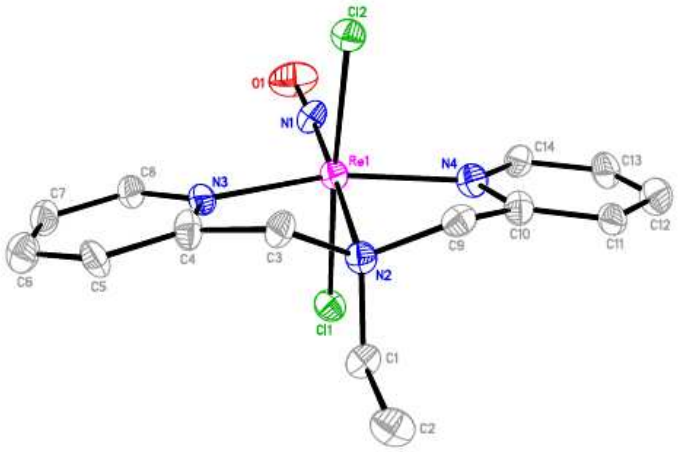


**Figure 5 –** ORTEP diagram of the $Re^I$-NO complex [$Re^ICl_2$(NO)(py-N(Et)-py)] in which the N3 ligand is coordinated in a meridional manner.

Similar in nature to the neutral, $Tc^I$-NO precursor [$Tc^ICl_2$(NO)(HOMe)($PPh_3$)$_2$] is the neutral, $Re^I$-NO precursor [$Re^ICl_2$(NO)($NCMe)_3$]. While the technetium species has two triphenylphosphine ligands that, by virtue of their steric bulk and the nature of the phosphine-technetium bond, can be difficult to replace, the rhenium complex has three acetonitrile ligands which are quite easy to replace. We employed these two structurally similar complexes in our attempt to synthesize directly analogous Tc(I) and Re(I) complexes of these ligands.

The reaction of [$Re^ICl_2$(NO)($NCMe)_3$] with this neutral, tridentate ligand yields the neutral Re(I) complex [$ReCl_2$(NO)(py-N(Et)-py)]. This species contains mutually *trans*-chloride ligands, with the tridentate ligand coordinated in a meridional manner. The nitrosyl ligand displays the expected multiple bonding throughout, with an Re-N bond length of 1.742(2) Å and nitrogen-oxygen bond length of 1.202(3) Å; and a nearly linear Re-N-O bond angle of 177.3(2)°. There is significant deviation from ideal octahedral geometry, mainly due to the small bite angle of the tridentate ligand. The Re-N bond length to the amine nitrogen *trans*- to the nitrosyl nitrogen is significantly longer than the bonds to the two aromatic amine nitrogens, as expected. {2.231(2) Å vs 2.085(2) and 2.091(2) Å}. Figure 5 displays an ORTEP diagram of *mer* [$ReCl_2$(NO)(py-N(Et)-py)]. Table 2 lists select bond lengths and angles from [$ReCl_2$(NO)(py-N(Et)-py)].

Continuing the evaluation of this structurally versatile family of ligands, we also examined reactions of the $Tc^I$-NO precursor

**Table 2** : Selected Bond Lengths (Å) and Angles (°) for the neutral $Re^I$-NO complex [$Re^ICl_2$(NO)(py-N(Et)-py)].

| | **Bond Lengths (Å)** | | **Bond Angles (°)** | | **Bond Angles (°)** |
|---|---|---|---|---|---|
| Re - N1 | 1.742(2) | O1 - N1 - Re | 177.3(2) | N3-Re-Cl1 | 86.99(7) |
| Re - N2 | 2.231(2) | Cl1 – Re - Cl2 | 175.29(2) | N4-Re-Cl1 | 91.68(7) |
| Re - N3 | 2.091(2) | N2 – Re - Cl2 | 90.38(6) | N1-Re-Cl1 | 92.64(8) |
| Re - N4 | 2.085(2) | N3 – Re - Cl2 | 89.73(7) | N3-Re-N2 | 78.97(8) |
| Re - Cl1 | 2.4262(7) | N4 – Re - Cl2 | 90.06(7) | N4-Re-N2 | 78.54(9) |
| Re - Cl2 | 2.4352(7) | N1 – Re - Cl2 | 91.41(8) | N1-Re-N2 | 176.88(10) |
| O1 - N1 | 1.202(3) | N2 – Re - Cl1 | 85.68(6) | N4-Re-N3 | 157.50(10) |
| | | N1 – Re - N3 | 103.59(10) | N1-Re-N4 | 98.90(10) |

$[Tc^{I}Cl_2(NO)(HOMe)\{PPh_3)_2]$ with the neutral tetradentate amine ligand (py-NH-NH-py). Here two major yellow products were identified and chromatographically separated. One cationic complex was $[Tc^{I}Cl(NO)(py\text{-}NH\text{-}NH\text{-}py)]Cl$ and it displays the chloride and nitrosyl ligands in a *cis*-orientation with the Tc -N-O bond angle of 172.3°. The second yellow product yielded green crystals upon standing in solution for an for crystalization. The X-ray structural determination showed them to also be a cationic $Tc^{I}$-NO complex, $[Tc^{I}Cl(NO)(PPh_3)(py\text{-}NH\text{-}NH\sim py)]^{+}$, which contains only three of the four nitrogen donors of the tetradentate ligand coordinated. We hypothesize that triphenylphosphine from the precursor eluted with the yellow product and eventually replaced the second chloride ligand during the prelude to crystalization, causing the yellow to green color change. The three coordinate tetradentate ligand displays one pyridine arm pendant, and the phosphine, chloride and nitrosyl ligands arranged in a *facial* manner. The Tc-N-O bond angle here was 176.3°. The structures of these two $Tc^{I}$-NO cationic complexes are displayed in Figure 6.

The $Re^{I}$-NO complex $[Re^{I}Br_2(NO)(NCMe)_3]$ reacts with the

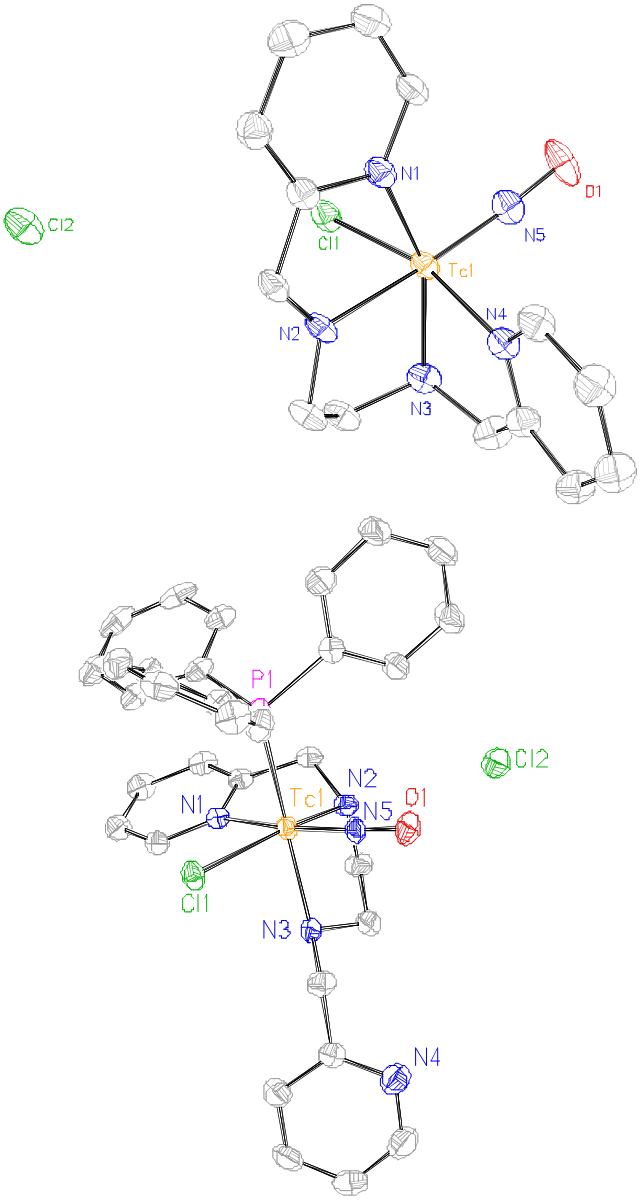


**Figure 6 –** ORTEP diagrams of the $Tc^{I}$-NO complex $[Tc^{I}Cl(NO)(py\text{-}NH\text{-}NH\text{-}py)]^{+}Cl^{-}$ and the cationic $Tc^{I}$-NO complex $[Tc^{I}Cl(NO)(PPh_3)(py\text{-}NH\text{-}NH\sim py)]^{+}Cl^{-}$.

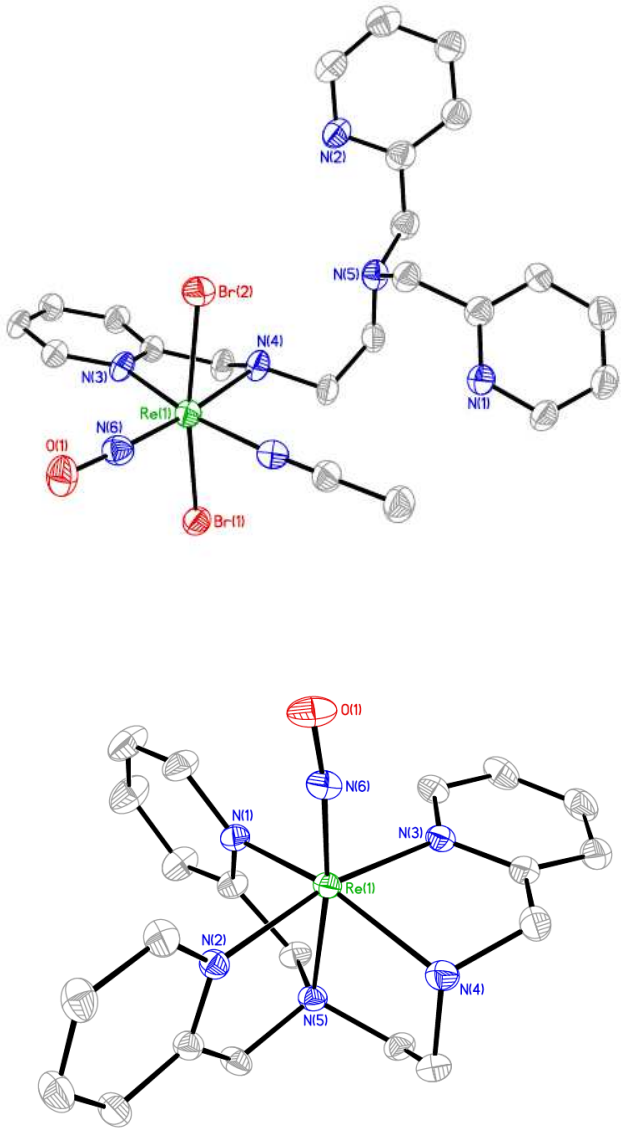


**Figure 7 –** ORTEP diagrams of the $Re^{I}$-NO complex $[ReBr_2(NO)\{py\text{-}CH_2NH\sim(CH_2CH_2N(CH_2\text{-}py\}_2]$, and the dicationic $Re^{I}$-NO complex $[Re(NO)(N_5)](BPh_4)_2$. The tetraphenylborate anions have been omitted from the dicationic complex for clarity.

**Table 3**

| Complex | M-N (Å) | N-O (Å) | M-N-O (°) | $A_t$* |
|---|---|---|---|---|
| $[TcCl_2(NO)(NCCH_3)(PPh_3)_2]$ | 1.781 (5) | 1.192(5) | 176.8(7) | Cl |
| $[TcCl_2(NO)(PNP_{pr})]$ *(mer)* | 1.751(5) | 1.163(6) | 177.9(4) | Cl |
| $[TcCl_2(NO)(PNP_{pr})]$ *(fac)* | 1.758(4) | 1.184(6) | 173.0(4) | N(R3)** |
| $[TcCl(NO)(SC_5H_4N)(PPh_3)_2]$ | 1.748(4) | 1.196(5) | 177.7(3) | N(py)** |
| $[Tc(NO)(SC_5H_4N)_2(PPh_3)]$ | 1.7497(12) | 1.1941(17) | 173.35(12) | N(py)** |
| $[Re(NO)(N_5)](BPh_4)_2]$ | 1.758(1) | 1.190(2) | 173.8(1) | Br |
| $[ReBr_2(NO)(NCMe)(N_5)]$ | 1.737(8) | 1.21(1) | 174.4(7) | Br |
| $[TcCl_2(NO)(N_3)]$ | 1.744(4) | 1.187(6) | 172.5(4) | N(R3)** |
| $[TcCl(NO)(N_3)(PPh_3)]Cl$ | 1.796(3) | 1.088(3) | 178.4(2) | Cl |
| $[TcCl(NO)(N_4)]Cl$ | 1.751(3) | 1.189(3) | 172.3(3) | N(R2)** |
| $[TcCl(NO)(N_4)(PPh_3)]Cl$ | 1.723(7) | 1.216(9) | 176.3(5) | N(py)** |
| $[ReBr_2(NO)(CH_3CN)_3]$ | 1.737(8) | 1.21(1) | 174.4(7) | Br |
| $[ReCl_2(NO)(N_3)]$ | 1.736(5) | 1.187(6) | 177.6(5) | N(R3)** |
| $[ReCl_2(NO)(N_3)]$ | 1.752(6) | 1.212(7) | 176.2(5) | N(R3)** |

* - $A_t$ = atom located *trans*- to the nitrosyl ligand

** - N(R2) = secondary amine, N(R3) = tertiary amine, N(py) = aromatic amine

potentially pentadentate-N5 ligand N1,N1,N2-tris(2-pyridinylmethyl)-1,2-ethanediamine in dichloromethane at room temperature to yield a mixture of a brown immobile species and a bright orange mobile species which were separated chromatographically. The orange species was determined to be $[ReBr_2(NO)\{py\text{-}CH_2NH\sim(CH_2CH_2N(CH_2\text{-}py\}_2]$, which contains the pentadentate ligand coordinated in a bidentate manner, with the three remaining amine moieties dangling in a pendant manner. This suggests that under the ambiant reaction conditions employed and in a non-polar solvent, the $Re^I$-NO precursor is more strongly bound to the halide ligands and the acetonitrile *cis*- to the nitrosyl core than was anticipated, a phenomenon previously reported for this rhenium complex. The analogous reaction in methanol yields the dicationic, fully chelated $Re^I$-NO species $[Re(NO)(N_5)](BPh_4)_2$. This dark brown species is precipitated from the methanol reaction mixture with addition of excess sodium tetraphenylborate. Figure 7 below displays the ORTEP diagrams for these two $Re^I$-NO complexes.

## 5. CONCLUSION

The established $Tc^{II}$- and $Re^{II}$-nitrosyl precursors $[M(NO)X_4]^-$ and $[M(NO)X_5]^{2-}$ form unstable reaction products which are very difficult to isolate cleanly. This isn't the case with the $M^I$-nitrosyl precursors. The results presented here establish that various the various bi-, tri-, tetra- and pentadentate ligands we have examined react effectively with the $Tc^I$-nitrosyl and $Re^I$-nitrosyl precursors. And depending on the chelate, form stable complexes incorporating various groups coordinated at the site *trans*- to the nitrosyl group. The presence of different donor groups at the site *trans*- to the nitrosyl group induce slight variations in the bending in the Tc-N-O bond. In fact the differences in M-N-O bond angle between a complex with a halide and an amine is at best marginal, and may reflect crystal packing forces rather than any inductive effect from the *trans*- ligand. See Table 3 above.

**ACKNOWLEDGEMENTS**

The X-ray Crystallographic Studies were performed in the MIT X-ray Diffraction laboratory of Dr. Peter Müller. The instrumentation, a Bruker X8 Kappa DUO four-circle diffractometer and a Bruker APEX2 CCD. were purchased with the help of funding from the National Science Foundation (NSF) under Grant Number CHE-0946721.

**6. REFERENCES**

[1] Agdeppa ED and Spilker ME. AAPS J., **2009**; 11(2): 286-299.

[2] Mariani G, Strauss HW. *Eur J Nucl Med Mol Imaging* **2011**; 38: 1189-1190

[3] Patton JA, Townsend DW, Hutton BF. *Semin Nucl Med* **2009**; 39:247-63.

[4] Buechel RR, Herzog BA, Husmann L, Burger IA, Pazhenkottil AP, Treyer V, Valenta I, von Schulthess P, Nkoulou R, Wyss CA, Kaufmann PA. *Eur J Nucl Med Mol Imaging*, **2010**; 37:773–8.

[5] Bocher M, Blevis IM, Tsukerman L, Shrem Y, Kovalski G, Volokh L. *Eur J Nucl Med Mol Imaging*, **2010**; 37:1887–1902.

[6] Seo Y, Mari C, Hasegawa BH. *Semin Nucl Med*, **2008**; 38:177-98.

[7] Yang YK, Yeh TL, Yao WJ, Lee IH, Chen PS, Chui NT, Lu RB. Psychiatry Res: *Neuroimaging*, **2008**; 162: 230-235.

[8] Mahmood A, Jones AG. Technetium radiopharmaceuticals. In: Welch MJ, Redvanly Cs, eds. *Handbook of Radiopharmaceuticals: Radiochemistry and Applications*. Chichester: John Wiley and Sons, **2003**: 323.

[9] Saha GB. *Fundamentals of Nuclear Pharmacy*., Sixth edition: **2010**; pp 83-127; Springer, NY.

[10] Alberto, R.; Schibli, R.; Waibel, R.; Abram, U.; Schubiger, A. P. *Coord. Chem. Rev*. **1999**; 190-192: 901-919.

[11] Alberto, R.; Schibli, R.; Schubiger, P. A. *J. Am. Chem. Soc*. **1999**; 121(25): 6076-6077.

[12] Dabrowiak J. Metals in Medicine. John Wiley & Sons, 2009; 262-263.

[13] Kramer, D. J.; Davison, A.; Davis, W. M.; Jones, A. G. *Inorg. Chem*. **2002**; 41(24): 6181–6183.

[14] He, H.; Morley, E. J.; Twamley, B.; Groeneman, H. R.; Bucˇ ar, D.-K.; MacGillivray R. L., Benny, D. P. *Inorg. Chem*. **2009**; 48(22): 10625–10634.

[15] Bowen, Meryn L.; Lim, Nathaniel C.; Ewart, Charles B.; Misri, Ripen; Ferreira, Cara L.; Hafeli, Urs; Adam, Michael J.; Orvig, Chris. *Dalton Trans*. **2009**; 42: 9216-9227.

[16] Lu G,; Maresca KP, Hillier SM, Zimmerman CN, Eckelman WC, Joyal JL, Babich JW. *Bioorg. Med. Chem Lett*. **2013**; 23: 1557-1563.

[17] Banerjee SR, Pullambhatla M, Foss CA, Falk A, Byun Y, Nimmagadda S, Mease RC, Pomper MG. *J. Med Chem*. **2013**; 56: 6108-6121.

[18] Sah B-R, Schibli R, Waibel R, von Boehmer L, Blauenstein P, Nexo E, Johayem A, Fischer E, Muller E, Soyka JD, Knuth AK, Haerle SK, Schubiger PA, Schaefer NG, Burger IA. *J. Nucl Med*. **2014**; 55: 43-49.

[19] Jurisson SS and Lydon JD. *Chem Rev*, **1999**; 99: 2205-2218.

[20] DeVries N, Cook J, Davison A, Nicholson T, Jones AG. *Inorg Chem*, **1989**; 29:1062-64.

[21] Gusev D, Llamazares A, Artus G, Jacobson H, Berke H. *Organomet*, **1999**;18:75-89.

[22] Cheah CT, Newman JL, Nowotnik DP, Thornback JR. *Nucl Med Biol*, **1987**; 14:573-77.

[23] Jiang Y, Blacquea O, Berke H. *Dalton Trans*. 2011; 40, 2578-87.

[24] Nicholson TL, Mahmood A, Limpa-Amara N, Salvarese N, Takase MK, Müller P, Akgun Z, Jones AG. *Inorg Chim Acta* **2011**; 373:301-05.

[25] Nicholson TL, Mahmood A, Akgun Z, Peng Y, Müller P, Jiang Y, Berke H, Jones AG. *Inorg Chim Acta*, **2013**; 405:455-60.

[26] Nicholson TL, Mahmood A, Müller P, Davison A, Storm-Blanchard S, Jones AG. *Inorg Chim Acta* **2010**; 365:484-86.

[27] Nicholson T, Hirsch-Kuchma M, Freiberg E, Davison A, Jones AG. *Inorg Chim Acta* **1998**;279:206-09.

[28] Blanchard SS, Nicholson TL, Davison A, Jones AG. *Inorg Chim Acta* **1997**; 254:225-31.

[29] Nicholson T, Mahmood A, Müller P, Refosco F, Tisato F, Jones AG. *Inorg Chim Acta* **2009**; 362:3637-40.